し、最終的にこれら寄生虫のオルガネラ機能を標的とする抗マラリア薬を開発する第一段階として、各オルガネラの分離を試みている。

赤血球内型マラリア原虫ミトコンドリアの呼吸鎖電子伝達系は化学療法剤の標的として期待されている。しかしマラリア原虫ミトコンドリアに関する情報は非常に限られたものであり、これが研究の進展を妨げている。一方、最近マラリア原虫には葉緑体と先祖を共有するアピコプラストと呼ばれる 35 kb の環状 DNA を持つオルガネラが存在し、マラリア原虫の増殖に必須な機能を有している事が判って来た。また、電子顕微鏡による観察から両者が細胞の中で常に近傍に局在している事が報告されている。そこで昨年の成果をふまえ、この２つのオルガネラの相互作用を調べ、さらにそれぞれの機能を独立に解析する目的で両者を分離できる方法を探索した。

またミトコンドリア機能の低下による原虫の増殖への影響をさらに詳細に調べる目的でヒトに感染する熱帯熱マラリア原虫に加え、ベクターである蚊のステージの原虫に関しても解析可能なネズミマラリア原虫 *Plasmodium berghei* について、TCA 回路系酵素でミトコンドリアのマーカー酵素でもあるコハク酸-ユビキノン還元酵素複合体（複合体 II）の遺伝子破壊株を作成してその影響を調べた。

（倫理面への配慮）

本研究はほとんどの部分が in vitro の実験系であり、倫理面の問題はない。またマウスのマラリア感染実験は共同研究を行っている自治医科大学の動物実験倫理規定に従って行った。

C. 研究結果

昨年度の結果を踏まえ、熱帯熱マラリア原虫の培養系から単離した粗ミトコンドリア画分を用い、ミトコンドリアとアピコプラストの相互作用を調べる目的で、パーコールの種類、遠心条件、添加剤など種々の処理、薬剤の効果を検討した。ミトコンドリアに関してはジヒドロオロト酸脱水素酵素、またアピコプラストに関しては 35Kb の環状 DNA 上の塩基配列を増幅する PCR を用いてその挙動を調べた。その結果、昨年はミトコンドリアとアピコプラストがパーコールによる遠心後に一部異なった位置に分離された程度であったが、今年度は Nocodazole を 10 μM、細胞破砕後に加えて粗ミトコンドリア画分を調製し、ここに Dnase I を添加する事、また Percoll PLUS を用いることにより大きく分離が改善された。その結果、ミトコンドリアとアピコプラスト両者を含む画分に加え、アピコプラストのみ

を含む画分を再現性良く調製する事が可能となった。

また複合体 II の触媒サブユニットであるフラボプロテインサブユニットの遺伝子破壊株を *P. berghei* を用いて作成し、赤血球内型および蚊のステージへの影響を調べた。前者ではほとんど影響がなかったのに対し、蚊のステージではオーキネトへの分化が 20%に低下し、オーシストの形成は全く見られなかった。また、遺伝子破壊株を吸血した蚊からは次の感染は全く起らなかった。さらに以上の研究を生化学的に進める事を可能にするため、ネズミマラリア原虫から大量のマラリア原虫を調製し、高活性、高純度のミトコンドリアを得る方法を確立した。

D. 考察

今回の結果から、これまで明確に分離できなかったマラリア原虫のミトコンドリアとアピコプラストに関し、アピコプラストのみを含む画分を得る事ができた点から、少なくともアピコプラストについては、より詳細な生化学的解析が可能となった。

また、TCA 回路と呼吸鎖を直接結ぶ複合体 II の遺伝子破壊がネズミマラリア原虫を用いた *in vivo* の実験系では赤血球内型には影響を与えず、蚊の体内のマラリア原虫の分化を阻害する事が判った点は、マラリア原虫のエネルギー代謝が生活環において大きく変動する事を示している。また、昨年培養系を用いた実験で報告した熱帯熱マラリア原虫ではこの遺伝子の破壊が増殖速度を低下させた点から考え、培養系の代謝は in vivo とは必ずしも一致していない事を示唆しており、今後のマラリア原虫の代謝研究に重要な知見と考えられる。

E. 結論

マラリア原虫やトリパノソーマ、またクリプトスポリジウムなど寄生原虫のミトコンドリアやアピコプラスト、最近その存在が明らかになって来たマイトソームなどのオルガネラは宿主哺乳類のそれと大きく異なった性質を持ち、その機能低下を通して化学療法の重要な標的となる事が明らかになった。

F. 健康危険情報

特になし

G. 研究発表

1. 論文発表

1) A cryptic algal group unveiled: a plastid biosynthesis pathway in the oyster parasite *Perkinsus marinus*. Matsuzaki M., Kuroiwa H., Kuroiwa T., Kita K. and Nozaki H. (2008) Mol. Biol. Evolution 25, 1167-1179

2) Malaria parasites reproduce with the same manner as flowering plants. Hirai M., Arai M., Mori T., Kawai S., Kita K., Kuroiwa T. and Matsuoka H. (2008) Current Biol. 18, 607-613
3) Coinfection with nonlethal murine malaria parasites suppresses pathogenesis caused by *Plasmodium berghei* NK65. Niikura M., Kamiya S., Kita K. and Kobayashi F. (2008) J. Immunol. 180, 6877-6884
4) Structures of *Trypanosoma cruzi* dihydroorotate dehydrogenase complexed with substrates and products: Atomic resolution insights into mechanisms of dihydroorotate oxidation and fumarate reduction. Inaoka, D. K., Sakamoto, K., Shimizu, H., Shiba T., Kurisu, G., Nara,T., Aoki, T., Kita, K. and Harada, S. (2008) Biochemistry 47, 10881-10891
5) Screening of detergents for solubilization, purification and crystallization of membrane proteins: a case study on succinate:ubiquinone oxidoreductase from *Escherichia coli*. Shimizu, H., Nihei, C., Inaoka, D. K., Mogi, T., Kita, K. and Harada, S. (2008) Acta Crystallographica F64, 858-862
6) Identification of New Inhibitors for Alternative NADH Dehydrogenase (NDH-II). Mogi, T., Matsushita, K., Murase, Y., Kawahara, Miyoshi, H., Ui, H., Shiomi, K., Ōmura, S. and Kita, K. (2009) FEMS Miclobiol. Lett. 291, 157-161
7) Mitochondrial Dehydrogenases in the Aerobic Respiratory Chain of the Rodent Malaria Parasite *Plasmodium yoelii yoelii*. Kawahara, K., Mogi, T., Tanaka, Q. T., Hata, M., Miyoshi, H. and Kita K. (2009) J. Biochem. 145, 229-237
8) Antibiotics LL-Z1272 identified as novel inhibitors discriminating bacterial and mitochondrial quinol oxidases. Mogi, T., Ui H., Shiomi, K., Ōmura, S., Miyoshi, H. and Kita, K. (2009) Biochim Biophys. Acta (Bioenergetics) 1787, 129-133
9) Fasting induced hypothermia and reduced energy production in mice lacking Acetyl-CoA Synthetase 2. Sakakibara, I., Fujino, T., Ishii, M., Tanaka, T., Shimosawa, T., Miura, S., Zhang, W., Tokutake, Y., Yamamoto, J., Awano, M., Iwasaki, S., Motoike, T., Okumura, M., Inagaki, T., Kita, K., Ezaki, O., Naito, M., Kuwaki, T., Chohnan, S., Yamamoto, T., Hammer, R. E., Kodama, T., Yanagisawa, M. and Sakai, J. (2009) Cell Metabolism 9, 191-202
10) Novel Mitochondrial Complex II Isolated from *Trypanosoma cruzi* is Composed of Twelve

Peptides Including a Heterodimeric Ip Subunit. Morales, J., Mogi, T., Mineki, S., Takashima, E., Mineki, R., Hirawake, H., Sakamoto, K., Ōmura, S. and Kita, K. (2009) J. Biol. Chem. 284, 7255-7263

2. 学会発表

1) 北 潔 寄生虫の生活環におけるダイナミックなエネルギー代謝の変動 第 81 回日本生化学会大会第・31 回日本分子生物学会年会 合同大会 平成 20 年 12 月

2) Madhavi Paranagama, Kimitoshi Sakamoto, Kiyoshi Kita *Ascaris suum* quinol fumarate reductase can produce high amount of reactive oxygen species. 第 81 回日本生化学会大会第・31 回日本分子生物学会年会 合同大会平成 20 年 12 月

3) Purification and crystallization of drug target trypanosome alternative oxidase (TAO) from *Trypanosoma brucei* Y. Kido, K. Sakamoto, S. Fujioka, M. Harada, D. Ohmori, F. Yamakura, H. Saimoto, Y. Yabu, T. Suzuki, S. Harada, K. Kita XVIIth International Congress for Tropical Medicine and Malaria 2008, Sept. Cheju, Korea

4) Novel subunit organization of the respiratory Complex II (succinate-ubiquinone oxidoreductase) in *Trypanosoma cruzi* Morales, J., Sakamoto, K., Kita, K. XVIIth International Congress for Tropical Medicine and Malaria 2008, Sept. Cheju, Korea

5) Toward anti-cryptosporidial chemotherapy by ascofuranone, specific and potent inhibitor against alternative oxidase (AOX)Harada, M., Fujimoto, Y., Nakamura, K., Kido, Y., Sakamoto, K., Yabu, Y., Suzuki, T., Yoshinari, S., Kita, K. XVIIth International Congress for Tropical Medicine and Malaria 2008, Sept. Cheju, Korea

H. 知的財産権の出願・登録状況

特になし

別紙３

厚生労働科学研究費補助金（医療機器開発推進研究事業）

分担研究報告書

リポーター遺伝子可視化プローブの開発

分担研究者　菊地和也　大阪大学大学院工学研究科教授

研究要旨
本研究において、酵素反応を受けることによりMRIコントラストが増大する機能性プローブの設計・合成を行い、リポーター遺伝子の発現をMRIにより検出するための新規原理を確立した。酵素反応の検出は、Gd^{3+}錯体により^{19}F-MRIのシグナル強度を制御するという原理に基づいている。この原理をリポーター遺伝子であるβ-galの検出に応用し、その酵素活性を^{19}F-MRIにより可視化することに成功した。

A．研究目的

酵素活性の*in vivo*での可視化は、基礎研究のみならず遺伝子治療などの医療応用にも関わる重要な技術であり現在大きな注目を集めている。MRIは、生体深部の断層画像を高い空間分解能で撮影することができる手法である。本研究では、MRIプローブにより酵素反応の可視化をするための原理を確立し、リポーター遺伝子の検出に応用した。

B．研究方法

生体内においてバックグラウンドシグナルがほとんどない観測核として^{19}Fを含む化合物をプローブに組み込み、特異的に^{19}Fのシグナル変化を捉えられるようにプローブの設計を行った。さらに、酵素反応によりMRIシグナルが変化するように、酵素により切断反応を受ける基質と、常磁性相互作用により^{19}Fのシグナルを減少させることのできるGd^{3+}錯体を^{19}F化合物に組み込んだプローブを作製した。

なお、酵素は、作用機構がよく理解されているカスパーゼとした。設計したプローブにより酵素反応を検出できるかどうかを^{19}F-NMR及び、^{19}F-MRIにより評価した。

次に、リポーター遺伝子産物であるβ-ガラクトシダーゼの検出に応用するために、上記プローブのペプチド部位をβ-ガラクトシダーゼの反応基質に変更した新規プローブを設計・合成した。β-ガラクトシダーゼの酵素活性の検出は、^{19}F-NMR及び^{19}F-MRIの測定により行った。

（倫理面への配慮）
特に必要なし

C．研究結果

カスパーゼ検出プローブの^{19}Fの緩和時間を測定したところ、正確に測定できないほどに、緩和時間が短縮されていることが示された。カスパーゼをプローブ試料に添加すると、プローブの^{19}Fの横緩和時間が増大しシャープなNMRシグナルが観測された。

さらに、^{19}F-MRIを撮像したところ、プローブ試料にカスパーゼを添加した場合のみ、MRIコントラストの増大が観測された(Mizukami *et al., J. Am. Chem. Soc.*, 2008; Mizukami *et al., Angew. Chem. Int. Ed.*, in press)。

次に、β-ガラクトシダーゼ検出プローブについて、緩和時間ならびにNMRスペクトルを測定したところ、緩和時間が短縮し、NMRシグナルが消失することが分かった。β-ガラクトシダーゼの添加により、NMRシグナルが回復し、^{19}F-MRIのコントラストも増大することが示された(Mizukami *et al.*, 未発表データ)。

D．考察

動物個体において、生きたまま遺伝子発現を検出する実用的な手法は、ほとんど開発されていない。MRIは、動物個体内の生体反応を追跡する優れた手法となると考え、本研究において、MRIにより酵素の活性を検出する原理の構築を行った。さらに、その原理を応用することで、遺伝子発現を可視化することのできるプローブの設計を行った。

MRIプローブの検出原理の確立のために、反応機構が良く知られた酵素であるカスパーゼをターゲットとしてプローブを設計した。カスパーゼとプローブの反応により緩和時間が変化しシャープなNMRシグナルが得られたことは、酵素反応前ではGd^{3+}との分子内常磁性相互作用により^{19}Fの緩和時間が短縮していたが、酵素反応によりプローブが切断され分子内常磁性相互作用が解消されたことを示している。この結果、^{19}F-MRIのコントラストも増大したと考えられる。

さらに、リポーター遺伝子であるβ-ガラクトシダーゼにも、同様の原理でプローブを設計することで、NMRによる検出が可能であることが分かった。また、β-ガラクトシダーゼとの反応により^{19}F-MRIのコントラストも明確に増大したことから、*in vivo*での可視化につながる重要な成果が得られたといえる。

E．結論

Gd^{3+}錯体による常磁性相互作用を利用することで、酵素反応を^{19}F-MRIにより検出する原理を構築し、リポーター遺伝子産物であるβ-ガラクトシダーゼの活性を検出することに成功した。

F．健康危険情報

特になし。

G．研究発表

1．論文発表

1. Mizukami, S., Tonai, K., Kaneko, M., **Kikuchi, K.** Lanthanide-Based Protease Activity Sensors for Time-Resolved Fluorescence Measurements. J. Am. Chem. Soc., 130, 14376-14377, 2008.

2. Mizukami, S., Takikawa, R., Sugihara, F., Shirakawa, M., **Kikuchi K.** Detection of Protease Activity using Dual-Function Fluorescence and ^{19}F MRI Spectroscopy. Angew. Chem. Int. Ed., *in press.*

3. Mizukami, S., Watanabe, S., Hori Y., and **Kikuchi, K.** Covalent Protein Labeling Based on Non-catalytic β-lactamase and a Designed FRET Substrate. J. Am. Chem. Soc., *in press.*

2．学会発表

1. **Kikuchi, K.** Chemical Sensor Molecules Which Convert Cellular Biological Responses to Chemical Output. (NIPS-JST International Workshop –From Photon to Mind–Advanced Nonlinear Imaging & Fluorescence-based Biosensors,

4.18-19, 2008, 岡崎）招待講演

2. **Kikuchi, K.** Chemical Sensor Molecules Which Convert Cellular Biological Responses to Chemical Output. (内藤コンフェレンス（ケミカルバイオロジー）, 9.9-12, 2008, 札幌) 招待講演

3. **Kikuchi, K.** Design, Synthesis and Application of Bio-imaging Probes Which Convert Biological Signals to Chemical Output. (ASBIC IV, 済州島, 韓国, 11.10-13, 2008) 招待講演

4. **Kikuchi, K.** Design, Synthesis and Application of Chemical Sensor Molecules Which Convert Biological Signals to Chemical Output. (Osaka University Forum, San Francisco, U.S.A., 12.8-10, 2008) 招待講演

5. **Kikuchi, K.** Development of Visualization Probes with Tunable Switches for Biological Applications. (G-COE国際シンポジウム, 1.13-14, 2009, 名古屋) 招待講演

6. **Kikuchi, K.** Designed MRI Probes with Enzyme Dependent Relaxation Time Modulatory Switches. (膜インタフェイス, 国際学会, 1.22-23, 2008, 豊中) 招待講演

7. **Kikuchi, K.** Design, Synthesis of Visualization Probes with Tunable Switches for Bio-imaging. (Gordon Research Conference, Metals in Biology, Ventura, U.S.A., 1.25-30, 2009) 招待講演

8. 菊地和也。生体機能を可視化する分子プローブのデザイン・合成・生物応用。（日本化学会第89春季年会,「生体模倣触媒」, 3. 29, 2009, 船橋）招待講演。

9. 菊地和也。可視化プローブのデザイン・合成による分子イメージング。（日日本化学会第89春季年会, ノーベル賞記念シンポジウム, 3. 28, 2009, 船橋）招待講演。

10. 菊地和也。緩和時間変化型MRIプローブのデザイン・合成・生物応用。（日本バイオイメージング学会第17回年会, 11. 1, 2008, 千葉）招待講演。

11. 菊地和也。化学プローブのデザイン・合成による生命現象の可視化解析。（高分子談話会, 10. 17, 2008, 大阪）招待講演。

12. 菊地和也。生体内の酵素活性を可視化する分子プローブのデザイン・合成・生物応用。（蛋白研研究会, 9. 25, 2008, 吹田）招待講演。

13. 菊地和也。生体内の酵素活性を可視化する分子プローブのデザイン・合成・生物応用。（第57回高分子討論会, 9. 24-26, 2008, 大阪）招待講演。

14. 菊地和也。錯体化学を応用した緩和時間変化型機能性MRIプローブ。（分子研研究会, 7. 18-19, 2008, 岡崎）招待講演。

15. 菊地和也。化学プローブのデザイン・合成による生体内機能分子の可視化解析。（新素材化学研究会第7回セミナー, 6. 6, 2008, 横浜）招待講演。

16. 菊地和也。*in vivo*イメージングを目指した可視化プローブ開発。（理化学研究所第2回「ケミカルバイオロジー領域」勉強会, 5. 23, 2008, ）招待講演。

H．知的財産権の出願・登録状況
（予定を含む。）
1．特許取得・申請
1．発明の名称：タンパク質を蛍光標識する方法，発明者：菊地和也，水上進，渡辺修司，出願番号：特願2008-273182，出願年月：2008年10月

2．実用新案登録
特になし

3．その他
特になし。

別紙３

厚生労働科学研究費補助金（医療機器開発推進研究事業）
分担研究報告書

認知活動感受性プロモーターの開発

分担研究者　奥野浩行　東京大学大学院医学系研究科・助教

研究要旨

神経細胞においてカルシウムシグナルは認知活動に相関した遺伝子発現活性化を引き起こす。この遺伝子活性化を個体動物においてリアルタイムで可視化するため、神経活動に依存した遺伝子発現レポーターを構築した。このレポーターシステムを①ウイルスベクターおよび②トランスジェニックマウスへと導入した。

A．研究目的

生体内カルシウムシグナリング破綻を計測する基盤技術の一つとして、カルシウムシグナル依存的な遺伝子発現をリアルタイムで計測するプローブ・レポーター分子を構築し、このレポーターを動物個体にする系の確立およびトランスジェニック動物の作成を目的とする。

B．研究方法

神経特異的前初期遺伝子*Arc*は、記憶課題負荷や感覚刺激等によって海馬や大脳新皮質においてカルシウムシグナルに依存的に発現誘導される。このArc遺伝子の発現制御領域を単離・解析し、この制御下に蛍光蛋白や発光蛋白を配置したレポーターを構築し、①ウイルスベクターへの応用および②トランスジェニック動物作成を行う。

（倫理面への配慮）

全ての動物実験および組換えDNA実験は、所属機関該当委員会の承認を得た上、機関ガイドラインを遵守し行った。

C．研究結果

培養神経細胞を用いた系を用いて詳細な *Arc* 遺伝子の発現機構解析を行った結果、神経特異性および活動依存性を規定するプロモーター領域の同定に成功した(Kawashima et al.,2009)。このプロモーターを利用したレポーターシステムを構築し、非侵襲的に活動依存的遺伝子発現を生きた神経細胞にて検出することに成功した(Kawashima et al.,2009)。このレポーターのウイルスベクター化にも成功した。さらに、トランスジェニックマウスを作出し、大脳において神経活動に相関したレポーター発現を検出に成功した。

D．考察

複数のトランスジェニックマウスの系統で、神経活動依存的なレポーターの発現上昇が確認された。特に蛍光タンパクをレポーターに持つトランスジェニックマウスでは生理的な感覚刺激（視覚・触覚）の他、探索行動などの認知活動に相関したレポーターの誘導が極めて再現的に観察され、これらマウスの有用性が示唆された。

E．結論

本研究による神経活動依存的な遺伝子発現の可視化法は、認知症をはじめとする神経疾患の病態の解明のための有用なツールとなる可能性が高い。

G．研究発表

1．論文発表

(1) Kawashima T, **Okuno H**, Nonaka M, Adachi-Morishima A, Kyo N, Okamura M, Takemoto-Kimura S, Worley PF and Bito H. (2009) . A synaptic activity-responsive element in the Arc/Arg3.1 promoter essential for synapse-to-nucleus signaling in activated neurons. *Proc. Natl. Acad. Sci. USA*, 106, 316-321.

(2) Bito H, Takemoto-Kimura S, **Okuno H.** (2008) Activity-dependent gene regulation: How do synapses talk to the nucleus and fine-tune neuronal outputs? in "Molecular Pain" p207-217, (M. Zhuo ed. Springer, New York)

(3) 尾藤晴彦、野中美応、布施俊光、藤井哉、竹本-木村さやか、**奥野浩行** (2008) シナプス機能とＰＳＤ構築を制御する分子機構. *蛋白質核酸酵素* 53, 418-423.

2．学会発表

国際学会

(1) **Okuno, H.**, Kawashima, T., Adachi-Morishima, A., Okamura, M., Worley, P., Bito, H. Critical genomic sequences for synaptic activity-dependent expression of the Arc gene. ***Soc. Neurosci. Abstr.*** 38.12, 第38回北米神経科学学会年会、2008. 11. 15-11. 19, Washington DC, USA. ポスター発表.

(2) Ageta-Ishihara, N., Takemoto-Kimura, S., Adachi-Morishima, A., Nonaka, M., **Okuno, H**., Bito H. Distinct regulation of cortical axonal and dendritic development by two Ca^{2+}-CaMKI pathways. ***Soc. Neurosci. Abstr***. 38.12, 第38回北米神経科学学会年会、2008. 11. 15-11. 19, Washington DC, USA, 口頭発表

(3) **Okuno H.**, Kawashima T, Nonaka M., Takemoto-Kimura S, Fujii H., Chowdhury S., Worley P.F., Bito H. Regulation of synaptic localization of Arc protein through interaction with Ca^{2+}/calmodulin-dependent kinase II beta. 6th FENS Forum 2008, 2008.7.12-7.16, Geneva, Switzerland, ポスター発表.

国内学会

(1) **Okuno H.**, Kawashima, T., Adachi-Morishima, A., Okamura, M., Bito, H. Synaptic activity-dependent regulation of neuronal immediate-early gene Arc/Arg3.1. 第３１回日本分子生物学会年会・第８１回日本生化学会大会（BMB2008），2008. 12. 9-12. 12、神戸、口頭発表およびポスター

(2) Ageta-Ishihara, N., Takemoto-Kimura, S., Adachi-Morishima, A., Nonaka, M., **Okuno, H.**, Bito H. Differential regulation of cortical dendritic and axonal development via distinct activation of CaMKK-CaMKI pathways, 第３１回日本分子生物学会年会・第８１回日本生化学会大会（BMB2008），2008. 12. 9-12. 12、神戸、口頭発表およびポスター

(3) **奥野　浩行**、川島　尚之、安達―森島　亜希、岡村　理子、尾藤晴彦. 可塑性関連遺伝子 Arc の活動依存的発現調節を担うゲノムエレメントの同定.. 第５１回日本神経化学会大会，2008. 9. 11-9. 13, 富山、口頭発表

(4) 上田（石原）　奈津実、竹本―木村　さやか、安達―森島　亜希、野中　美応、**奥野　浩行**、尾藤　晴彦. 異なる CaMKK-CaMKI 経路による軸索/樹(状突起の特異的形成制御，第５１回日本神経化学会大会，2008. 9. 11-9. 13, 富山、口頭発表

(5)Kawashima, T., Okuno, H., Okamura, M., Bito, H. A novel synaptic activity-responsive element of the Arc promoter, 第３１回日本神経科学大会（Neuroscience 2008)、2008. 7. 9-7. 11，東京、口頭発表

(6) Ageta-Ishihara, N., Takemoto-Kimura, S., Adachi-Morishima, A., Nonaka, M., Okuno, H., Bito H. Differential roles of CaMKIgamma; and CaMKIalpha; in cortical dendritic and axonal development. 第３１回日本神経科学大会（Neuroscience 2008)、2008. 7. 9-7. 11，東京、口頭発表.

H．知的財産権の出願・登録状況
（予定を含む。）

1．特許取得・申請
特になし

2．実用新案登録
特になし

3. その他
特になし。

別紙4

研究成果の刊行に関する一覧表

書籍

著者氏名	論文タイトル名	書籍全体の編集者名	書　籍　名	出版社名	出版地	出版年	ページ
尾藤晴彦、有賀純	神経細胞内ではたらくシグナル伝達.	古市貞一	分子・細胞・シナプスからみる脳	東京大学出版会	東京	2008	131-180
Bito, H., Takemoto-Kimura, S., & **Okuno, H.**	Activity-dependent gene regulation: How do synapses talk to the nucleus and fine-tune neuronal outputs?	M. Zhuo	*Molecular Pain*	Springer	New York	2008	207-217

雑誌

発表者氏名	論文タイトル名	発表誌名	巻号	ページ	出版年
Kawashima T, **Okuno H**, Nonaka M, Adachi-Morishima A, Kyo N, Okamura M, Takemoto-Kimura S, Worley PF, **Bito H**.	A synaptic activity-responsive element in the Arc/Arg3.1 promoter essential for synapse-to-nucleus signaling in activated neurons.	*Proc. Natl. Acad. Sci. USA.*	**106**	316-321	2009
尾藤晴彦、野中美応、布施俊光、藤井哉、竹本-木村さやか、**奥野浩行**	シナプス機能とＰＳＤ構築を制御する分子機構.	*蛋白質核酸酵素*	**53**	218-228	2008
Matsuzaki M., Kuroiwa H., Kuroiwa T., **Kita K.**, Nozaki H	A cryptic algal group unveiled: a plastid biosynthesis pathway in the oyster parasite *Perkinsus marinus*	*Mol. Biol. Evolution*	**25**	1167-1179	2008

Hirai M., Arai M., Mori T., Kawai S., **Kita K.**, Kuroiwa T., Matsuoka H.	Malaria parasites reproduce with the same manner as flowering plants	*Current Biol*	**18**	607-613	2008
Niikura M., Kamiya S., **Kita K.**, Kobayashi F	Coinfection with nonlethal murine malaria parasites suppresses pathogenesis caused by *Plasmodium berghei* NK65	*J. Immunol*	**180**	6877-6884	2008
Inaoka, D. K., Sakamoto, K., Shimizu, H., Shiba T., Kurisu, G., Nara,T., Aoki, T., **Kita, K.**, Harada, S	Structures of *Trypanosoma cruzi* dihydroorotate dehydrogenase complexed with substrates and products: Atomic resolution insights into mechanisms of dihydroorotate oxidation and fumarate reduction	*Biochemistry*	**47**	10881-10891	2008
Shimizu, H., Nihei, C., Inaoka, D. K., Mogi, T., **Kita, K.**, Harada, S	Screening of detergents for solubilization, purification and crystallization of membrane proteins: a case study on succinate:ubiquinone oxidoreductase from *Escherichia coli*.	*Acta Crystallographica*	**F64**	858-862	2008
Mogi, T., Ui H., Shiomi, K., Ōmura, S., Miyoshi, H. , **Kita, K.**	Antibiotics LL-Z1272 identified as novel inhibitors discriminating bacterial and mitochondrial quinol oxidases.	*Biochim Biophys. Acta (Bioenergetics)*	**1787**	129-133	2009
Kawahara, K., Mogi, T., Tanaka, Q. T., Hata, M., Miyoshi, H., **Kita K**.	Mitochondrial Dehydrogenases in the Aerobic Respiratory Chain of the Rodent Malaria Parasite *Plasmodium yoelii yoelii*	*J. Biochem*	**145**	229-237	2009

Mogi, T., Matsushita, K., Murase, Y., Kawahara, Miyoshi, H., Ui, H., Shiomi, K., Ōmura, S. , **Kita, K.**	Identification of New Inhibitors for Alternative NADH Dehydrogenase (NDH-II).	*FEMS Miclobiol. Lett*	**291**	157-161	2009
Morales, J., Mogi, T., Mineki, S., Takashima, E., Mineki, R., Hirawake, H., Sakamoto, K., Ōmura, S., **Kita K.**	Novel Mitochondrial Complex II Isolated from *Trypanosoma cruzi* is Composed of Twelve Peptides Including a Heterodimeric Ip Subunit	*J. Biol. Chem.*	**284**	7255-7263	2009
Sakakibara, I., Fujino, T., Ishii, M., Tanaka, T., Shimosawa, T., Miura, S., Zhang, W., Tokutake, Y., Yamamoto, J., Awano, M., Iwasaki, S., Motoike, T., Okumura, M., Inagaki, T., Kita, K., Ezaki, O., Naito, M., Kuwaki, T., Chohnan, S., Yamamoto, T., Hammer, R. E., Kodama, T., Yanagisawa, M., Sakai, J.	Fasting induced hypothermia and reduced energy production in mice lacking Acetyl-CoA Synthetase 2	*Cell Metabolism*	**9**	191-202	2009
Mizukami, S., Tonai, K., Kaneko, M., **Kikuchi, K.**	Lanthanide-Based Protease Activity Sensors for Time-Resolved Fluorescence Measurements.	*J. Am. Chem. Soc.*	**130**	14376-14377	2008

Mizukami, S., Watanabe, S., Hori Y.,**Kikuchi, K.**	Covalent Protein Labeling Based on Non-catalytic β-lactamase and a Designed FRET Substrate.	**J. Am. Chem. Soc.**			in press
Mizukami, S., Takikawa, R., Sugihara,F., Shirakawa, M., **Kikuchi K.**	Detection of Protease Activity using Dual-Function Fluorescence and ^{19}F MRI Spectroscopy.	**Angew. Chem. Int. Ed.**			in press

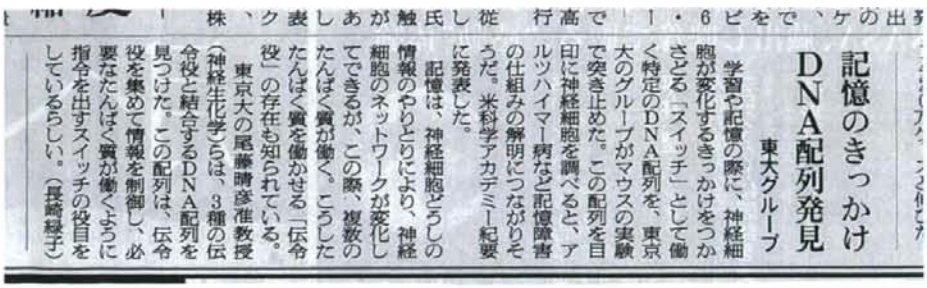

記憶のきっかけ DNA配列発見

東大グループ

学習や記憶の際に、神経細胞が変化するきっかけをつかさどる「スイッチ」として働く特定のDNA配列を、東京大のグループがマウスの実験で突き止めた。この配列を目印に神経細胞を調べると、アルツハイマー病など記憶障害の仕組みの解明につながりそうだ。米科学アカデミー紀要に発表した。

記憶は、神経細胞どうしの触情報のやりとりにより、神経細胞のネットワークが変化してできるが、この際、複数のたんぱく質が働く。こうしたたんぱく質を働かせる「伝令役」の存在も知られている。

東京大の尾藤晴彦准教授（神経生化学）らは、3種の伝令役と結合するDNA配列を見つけた。この配列は、伝令役を集めて情報を制御し、必要なたんぱく質が働くように指令を出すスイッチの役目をしているらしい。（長崎緑子）

朝日新聞
2009年1月15日　夕刊9面掲載

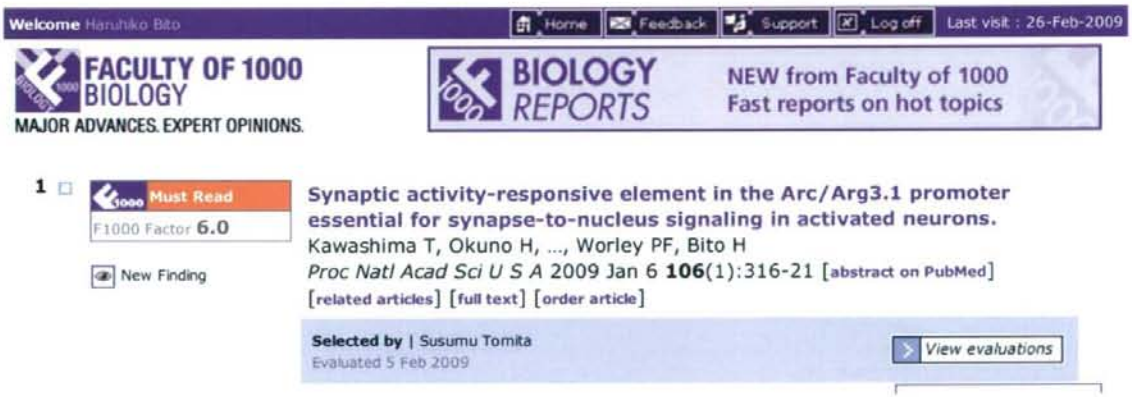

最も権威ある論文ピアレビューサイトである F1000 Biology にて Must Read（必読）論文として 2009 年 2 月 5 日付けで紹介

Synaptic activity-responsive element in the *Arc/Arg3.1* promoter essential for synapse-to-nucleus signaling in activated neurons

Takashi Kawashima[a,1], Hiroyuki Okuno[a,1,2], Mio Nonaka[a], Aki Adachi-Morishima[a], Nan Kyo[a], Michiko Okamura[a], Sayaka Takemoto-Kimura[a], Paul F. Worley[b], and Haruhiko Bito[a,c,2]

[a]Department of Neurochemistry, Graduate School of Medicine, University of Tokyo, Bunkyo-ku, Tokyo 113-0033, Japan; [c]CREST-JST, Kawaguchi, Saitama 332-0012, Japan; and [b]Department of Neuroscience, Johns Hopkins University School of Medicine, Baltimore, MD 21205

Edited by Yoshito Kaziro, Kyoto University, Kyoto, Japan, and approved November 17, 2008 (received for review July 14, 2008)

The neuronal immediate early gene *Arc/Arg-3.1* is widely used as one of the most reliable molecular markers for intense synaptic activity in vivo. However, the *cis*-acting elements responsible for such stringent activity dependence have not been firmly identified. Here we combined luciferase reporter assays in cultured cortical neurons and comparative genome mapping to identify the critical synaptic activity-responsive elements (SARE) of the *Arc/Arg-3.1* gene. A major SARE was found as a unique ≈100-bp element located at >5 kb upstream of the *Arc/Arg-3.1* transcription initiation site in the mouse genome. This single element, when positioned immediately upstream of a minimal promoter, was necessary and sufficient to replicate crucial properties of endogenous *Arc/Arg-3.1*'s transcriptional regulation, including rapid onset of transcription triggered by synaptic activity and low basal expression during synaptic inactivity. We identified the major determinants of SARE as a unique cluster of neuronal activity-dependent *cis*-regulatory elements consisting of closely localized binding sites for CREB, MEF2, and SRF. Consistently, a SARE reporter could readily trace and mark an ensemble of cells that have experienced intense activity in the recent past in vivo. Taken together, our work uncovers a novel transcriptional mechanism by which a critical 100-bp element, SARE, mediates a predominant component of the synapse-to-nucleus signaling in ensembles of Arc/Arg-3.1-positive activated neurons.

immediate-early genes | MEF2 | SRF | calcium | CREB

Fine tuning of gene expression and protein translation in mature neurons is of vital importance to brain function (1). Aberrance of adaptive responses such as long-term memory or late-phase synaptic plasticity has indeed been the hallmark of several genetically engineered mouse mutants in which the expression or the function of key transcription factors have been altered (2, 3). Thus it appears that the supply of neuronal proteins must be tightly matched to the cellular demand at any given time, to maintain proper neuronal circuit function.

One critical determinant of neuronal gene expression is the neuron's own activity. Dramatic changes in gene expression have been reported upon robust reorganization of sensory information processing (such as during critical period plasticity of the visual cortex), or through characteristic cognitive processes (such as establishment of long-term memory) (4–6). Barrages of synaptic activity that alters synaptic strength can directly up- or downregulate various constituents of the synaptic machinery and many signaling molecules (7–9). Studies of the transcriptional activation mechanisms leading to upregulation of the immediate early genes c-*fos*, *zif*268, and of the brain-derived neurotrophic factor (BDNF) indicated that transcription factors such as the Ca^{2+}/cAMP-response element binding protein (CREB) and the serum response factor (SRF) may play a privileged role as key neuronal activity sensors in the nucleus (10–12).

An activity-regulated cytoskeleton-associated protein (Arc/Arg-3.1) has recently emerged as an attractive candidate effector molecule/immediate early gene product (13, 14), whose induction may correlate, at least in part, with the induced synaptic alteration phenotype (15–18). Furthermore, *Arc/Arg-3.1* transcription is induced extremely rapidly and *Arc/Arg-3.1* mRNA detection, by fluorescence in situ hybridization, has now been validated as a reliable trace of intense synaptic activity within a neuronal ensemble in the hippocampus (e.g., during novelty exposure), in the amygdala (e.g., during acquisition of long-term fear memory), or in the sensory cortices (e.g., after intense sensory experience following sensory deprivation) (19–22). Despite the growing interest in Arc/Arg-3.1 function, however, surprisingly little is yet known about the genomic mechanism by which acute delivery of synaptic information can be reliably encoded into *Arc/Arg-3.1* transcriptional events in the nucleus. To address this question, we investigated the *cis*-acting enhancer elements responsible for such stringent neuronal activity dependence.

Results

Presence of a Strong Synaptic Activity-Responsive Element in a Distal Portion of the Mouse *Arc/Arg-3.1* Promoter. We performed transcriptional reporter assays using primary culture neurons in which endogenous *Arc/Arg-3.1* is rapidly and transiently induced by 4AP/BIC stimulation (Fig. 1*A*). In the mouse genome, 7 conserved regions exceeding 65% identity per 100 bp with humans were found between 0 and −5 kb (from the transcription initiation site), and 1 distal region was mapped between −6 kb and −7 kb (Fig. 1*B*). No further conserved regions were found between −7 kb and −10 kb.

Prior studies have demonstrated the role of a proximal region (<2 kb) of the *Arc/Arg-3.1* promoter in its activity dependence (23, 24). Consistent with this, proximal regions [Arc1000 (−996 to +198) and Arc2000 (−1996 to +198)] showed 2- to 3-fold induction after stimulation in our assays (Fig. 1*C*). Genomic regions up to 3 kb (Arc3000, −2996 to +198) conferred an 8-fold induction (Fig. 1*C*). The activated levels of 4-kb and 5-kb fragments [Arc4000 (−3996 to +198) and Arc5000 (−4996 to +198)] were similar to that of Arc3000, but their basal levels in TTX were significantly lower than those of Arc1000, Arc2000, and Arc3000 ($P < 0.01$), resulting in an ≈20-fold induction (Fig. 1*C*). Unexpectedly, extension of the genomic sequence up to 7 kb (Arc7000, −7065 to +198) resulted in further increase in its induction ability, of >150-fold, in

Author contributions: H.O. and H.B. designed research; T.K., H.O., M.N., and N.K. performed research; A.A.-M., M.O., S.T.-K., and P.F.W. contributed new reagents/analytic tools; T.K., H.O., M.N., N.K., and H.B. analyzed data; and T.K., H.O., M.N., and H.B. wrote the paper.

The authors declare no conflict of interest.

This article is a PNAS Direct Submission.

[1]T.K. and H.O. contributed equally to this work.

[2]To whom correspondence may be addressed. E-mail: hbito@m.u-tokyo.ac.jp or okuno@m.u-tokyo.ac.jp.

This article contains supporting information online at www.pnas.org/cgi/content/full/0806518106/DCSupplemental.

© 2008 by The National Academy of Sciences of the USA

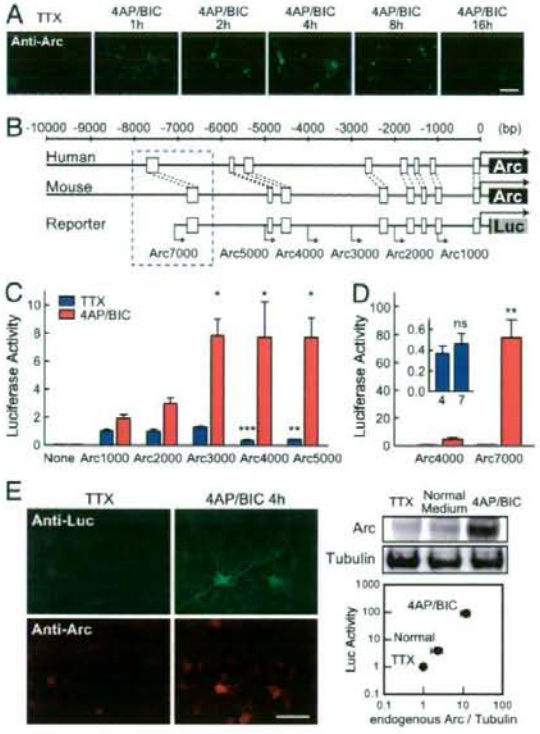

Fig. 1. Multiple regulatory elements in the mouse *Arc/Arg-3.1* promoter. (*A*) Time course of endogenous Arc/Arg-3.1 protein induction by 4AP/BIC stimulation. Cultured cortical neurons pretreated with TTX were stimulated with 4AP/BIC for indicated hours. (Scale bar, 100 μm.) (*B*) Evolutionarily conserved genomic regions in the upstream of the *Arc/Arg-3.1* gene. Regions conserved between mice and humans are shown as white boxes. A destabilized luciferase (Luc-PEST) gene was used as a reporter. (*C*) Transcriptional regulatory activities of Arc1000–5000. Cultured cortical neurons were stimulated with 4AP/BIC for 4 h. Luciferase activities are normalized relative to the activity of Arc1000 under the TTX treatment. This normalization applies to all luciferase assay data in this study. Statistical analyses were performed separately for the TTX and 4AP/BIC data sets. $n = 5$ independent experiments. *, $P < 0.05$; **, $P < 0.01$; ***, $P < 0.001$ compared with the TTX or the 4AP/BIC value of Arc1000 (1-way ANOVA with Tukey's test). (*D*) Strong activation ability of Arc7000. The *y* axis for the basal levels were expanded and shown in the inset for clarity. $n = 7$ independent experiments. **, $P < 0.01$; ns, not significant (paired *t* test) compared with the 4AP/BIC or the TTX value of Arc4000. (*E*) Arc7000-driven luciferase correlates with endogenous Arc induction. *Left*, coexpression of luciferase and endogenous Arc protein after stimulation. (Scale bar, 50 μm.) *Right*, simultaneous quantification of luciferase activities and endogenous Arc protein levels in the same samples. Cell lysates were prepared from neurons with no treatment (normal medium), with TTX, or with 4AP/BIC for 4 h. Arc protein levels were quantified by Western blotting and plotted against the reporter luciferase activities. Duplicated samples were analyzed and shown.

response to stimulation ($P < 0.01$) (Fig. 1*D*), indicating the presence of a very potent enhancer in the most distal conserved region.

We also examined the relative potency of Arc7000 at single-cell resolution, using a destabilized GFP as a fluorescent reporter. As expected from the results of luciferase assays, GFP signals in individual neurons were more elevated downstream of Arc7000 than of Arc4000 ($P < 0.001$) [supporting information (*SI*) Fig. S1]. Additionally, no GFP signals were detected in glial cells (data not shown), indicating that Arc7000 may also determine the neuron-specific expression pattern of the *Arc/Arg-3.1* gene.

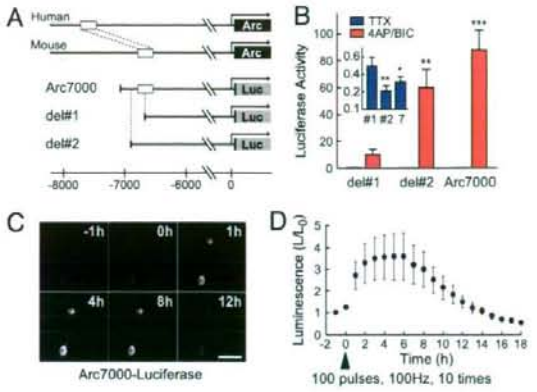

Fig. 2. The distal conserved region is crucial for the Arc7000 promoter activity. (*A*) Arc7000 deletion mutants. The genomic locus framed by a dashed box in Fig. 1 *B* is expanded and shown. (*B*) Presence of a potent enhancer element between Arc7000-del no. 1 and Arc7000-del no. 2. $n = 6$ independent experiments. *, $P < 0.05$; **, $P < 0.01$; ***, $P < 0.001$, compared with the TTX or the 4AP/BIC value of Arc7000-del no. 1 (1-way ANOVA with Tukey's test). (*C* and *D*) Rapid and transient induction of luciferase luminescence by Arc7000 after high-frequency electrical stimulation. Hippocampal neurons transfected with a click beetle luciferase (ELuc) vector was electrically stimulated at 0 h (triangle), and luminescence in the soma was monitored. Representative images were shown in *C*. $n = 9$ neurons. (Scale bar, 50 μm.)

The Arc7000 activity correlated well with the endogenous *Arc/Arg-3.1* expression, because the reporter luciferase after stimulation was mostly coexpressed in the same cells as endogenously induced Arc/Arg-3.1 (Fig. 1*E*), and Western blots showed a linear relation between luciferase activity and endogenous Arc protein levels (Fig. 1*E*).

Identification of a Synaptic Activity-Responsive Element (SARE) in Arc7000 That Is Critical for Activity-Regulated Gene Expression. To pin down the critical enhancer element, we next examined a genomic deletion (del) mutant Arc7000-del no. 1 (−6667 to +198), in which the most distal conserved region was truncated (Fig. 2*A*). This mutant revealed a striking decrease in activity dependence compared with Arc7000 ($P < 0.01$) (Fig. 2*B*). In contrast, Arc7000-del no. 2 (−6893 to +198), in which the conserved region was spared, possessed an activity dependence indistinguishable from Arc7000 (Fig. 2 *A* and *B*). Intriguingly, the basal level of Arc7000-del no. 2 in TTX was indistinguishable from that of Arc7000, but was significantly lower than that of Arc7000-del no. 1 ($P < 0.05$) (Fig. 2*B*).

We then tested whether robust high-frequency synaptic activity triggered by electrical stimulation could induce reporter gene expression downstream of Arc7000 in single neurons. Hippocampal neurons transfected with an Arc7000-ELuc-PEST plasmid were stimulated with field electrical pulses. In responding neurons, luminescence started to increase immediately after the stimulation, reached plateau after 4–6 h, and attenuated gradually after 8 h (Fig. 2 *C* and *D*). This activation time course closely resembled the induction time course of endogenous *Arc/Arg-3.1* following electrical stimulation in vivo (25).

These findings were most consistent with the presence of a potent enhancer, which we termed SARE, in a region between Arc7000-del no. 1 and Arc7000-del no. 2 (Fig. 2 *A* and *B*). Close examination of the evolutionarily conserved region present in del no. 2 but truncated in del no. 1 revealed a series of short conserved sequence stretches, of ≈100 bp (Fig. 3*A*).

To directly test the role of these sequence stretches, we fused a 104-bp fragment (−6793 to −6690) to a TATA-containing short

NEUROSCIENCE

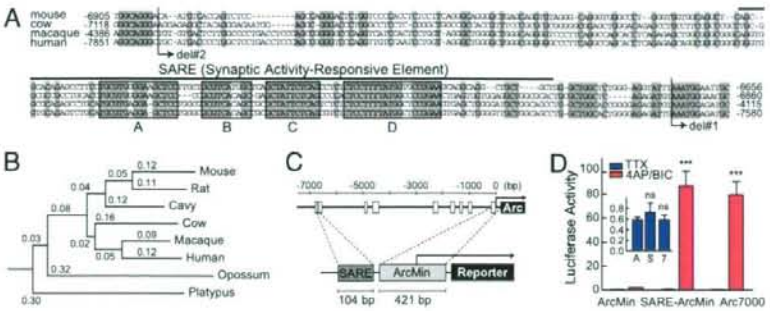

Fig. 3. *Arc/Arg-3.1* SARE replicates Arc7000 promoter activity. (*A*) Comparison across multiple mammalian species. Conserved sequences were highlighted in gray. A short stretch of sequences (thick line) consisted of 4 highly conserved boxes (boxes *A–D*) was termed a synaptic activity responsive element (SARE). (*B*) Dendrogram showing the divergence of SARE sequences across various mammalian species. The numbers represent the branch length, which indicates the degree of nucleotide differences. Detailed nucleotide information for this analysis is shown in Fig. S3. (*C*) SARE-ArcMin reporter vector. SARE was fused directly upstream of ArcMin, a TATA-containing sequence around the transcription initiation site of the *Arc/Arg-3.1* gene. (*D*) SARE-ArcMin replicates the activation ability of Arc7000. $n = 5$ independent experiments. ***, $P < 0.001$; ns, not significant, compared with the TTX or the 4AP/BIC value of ArcMin (1-way ANOVA with Tukey's test).

promoter (−222 to +198) of the *Arc/Arg-3.1* gene (SARE-ArcMin) (Fig. 3 *A* and *C*). Luciferase activity driven by SARE-ArcMin was increased >100-fold in response to stimulation (Fig. 3*D*). The basal levels did not differ between SARE-ArcMin and ArcMin (Fig. 3*D*). Importantly, the activation level of SARE-ArcMin was indistinguishable from that of Arc7000 (Fig. 3*D*). The fluorescent protein reporter assay also revealed a dramatic increase in GFP signal positivity in SARE-ArcMin reporter-transfected neurons, following synaptic stimulation in individual cells (Fig. S2). None of the other conserved genomic regions showed such strong enhancer activities on their own (data not shown).

Taken together, these results indicate the existence of a novel SARE in the distal *Arc/Arg-3.1* promoter, which appeared to be critical for replicating the amplitude of activity-induced transcriptional response of the full promoter in the absence of any other adjacent genomic regions, when placed immediately upstream of the minimal *Arc/Arg-3.1* promoter.

Contribution of 3 Activity-Regulated Transcription Factors, CREB, MEF2, and SRF, in SARE Activation. SARE contained 4 conserved sequence stretches (Fig. 3*A*). This raised the possibility that perhaps distinct transcription factors could in principle bind to SARE, and thus, these putative binding sites were tentatively called boxes *A*−*D* (Fig. 3*A*). All 4 boxes were conserved in most mammals, except some species such as the opossum and the platypus (Fig. 3*B* and Fig. S3). To address their requirements, we introduced mutations in each of these boxes, and tested them either in the upstream of a TATA-containing minimal CMV promoter (minCMV, which has virtually no transcriptional activity per se), or in the context of the full Arc7000 promoter (Fig. 4 *A* and *B*). Luciferase activity of SARE-minCMV was increased >80-fold in response to stimulation, and this induction was dramatically diminished by single mutations in boxes *B*, *C*, and *D* ($P < 0.001$). In contrast, a mutation in box *A* had no significant effect (Fig. 4*A*). Combined mutations in both boxes *B* and *D* almost completely blocked the induction (Fig. 4*A*). Similar results were obtained in the context of the full Arc7000 promoter (Fig. 4*B*). These data suggested that boxes *B*, *C*, and *D* were required for the enhancer activity of SARE, and some cooperativity might exist between them. Additionally, the basal level of SARE-minCMV was significantly elevated by mutating box *D* ($P < 0.001$) (Fig. 4*A*), indicating that box *D* might also contribute to attenuating transcription during synaptic inactivity.

We next sought to identify the transcription factors that bound to these sites. Box *B* contained a sequence matching a half site of the consensus binding sequence for CREB (Fig. 4*C*). Box *C* matched the consensus for myocyte enhancer factor 2 (MEF2) with the exception of 2 nucleotides (Fig. 4*C*). The 5′-end of box *D* perfectly matched the consensus for SRF, while the 3′-end perfectly matched the consensus for the ternary complex factors (TCFs), the well-characterized accessory proteins of SRF (Fig. 4*C*). An electrophoretic mobility-shift assay (EMSA) revealed the formation of each specific protein-DNA complex for boxes *B*, *C*, and *D* in nuclear extracts obtained from electroconvulsive shock-treated rat cortices (Fig. 4*C*). Consistent with the consensus sequence matches, each complex was disrupted by adding excess amounts of competitor DNA, and gel supershifts were detected using CREB-, MEF2-, and SRF-specific antibodies. Furthermore, chromatin immunoprecipitation (ChIP) assay using neuronal culture confirmed physical binding of CREB, MEF2, and SRF to SARE in cultured neurons (Fig. 4*D* and Fig. S4). Together, these data strongly suggest that CREB, MEF2, and SRF play critical roles in SARE activation via binding to boxes *B*, *C*, and *D*, respectively (Fig. 4*C*).

We further investigated the intracellular signaling pathways upstream of these transcription factors. The SARE activation in the context of Arc7000 by 4AP/BIC treatment was almost completely suppressed when both AMPA-R and NMDA-R were blocked, confirming that excitatory synaptic inputs trigger the activation (Fig. S5*A*). In addition, the activation was reduced 80% when only NMDA-R was blocked, indicating that synaptic Ca^{2+} influx through NMDA-R is critical for the SARE activation (Fig. S5*A*). The activation was also significantly diminished by KN-93, a Ca^{2+}/calmodulin-dependent protein kinase (CaMK) inhibitor, and U0126, a mitogen-activated protein kinase kinase (MEK) inhibitor (Fig. S5*B*). An essentially similar pharmacological profile was obtained when the SARE activity was tested in the upstream of the minimal CMV promoter (Fig. S5*C*). These results confirmed that SARE was crucial for a large part of the transcriptional response of the *Arc/Arg-3.1* gene that lied downstream of activity-regulated signaling mechanisms, such as CaMK and MAPK cascades, both of which were previously shown to underlie many aspects of neuronal adaptive responses (8, 26).

Visualization of Activated Cells in a Neuronal Circuit Using a SARE Reporter Lentivirus Vector. One potential caveat of the above experiments was that these in vitro assays did not involve genomic integration of the reporter genes. Therefore, we designed a lentivirus-based gene delivery system to introduce SARE-driven reporters into the neuronal genome (Fig. 5). We constructed a lentivirus vector containing 2 expression cassettes placed in opposite directions and separated by an insulator sequence. In 1 cassette,

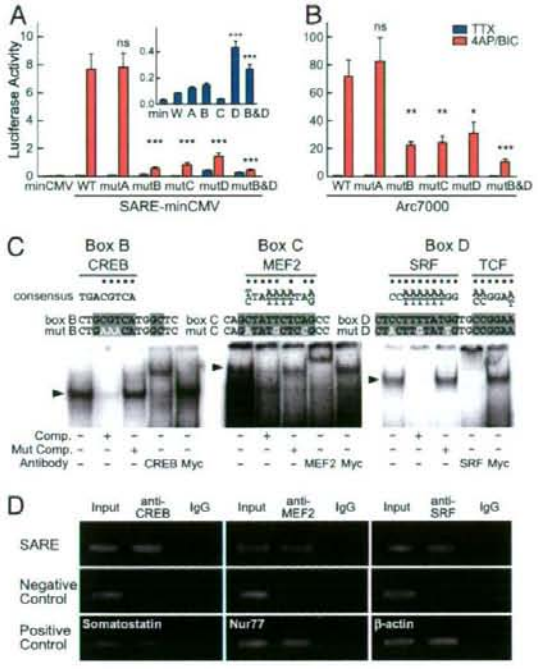

Fig. 4. Involvement of coclustered CREB, MEF2, and SRF in the SARE activation. (*A*) Loss of the SARE activity by mutations in the boxes *B*, *C*, and *D*, but not *A*, in the context of a minimal CMV promoter (SARE-minCMV). Note that the basal level (TTX) was elevated by a mutation in the box *D* (inset). WT, wild-type; ***, $P < 0.001$; ns, not significant, compared with the TTX or the 4AP/BIC value of WT (1-way ANOVA with Tukey's test). (*B*) Loss of the Arc7000 activity by mutations in the boxes *B*, *C*, and *D*. WT, wild-type; *, $P < 0.05$; **, $P < 0.01$; ***, $P < 0.001$; ns, not significant, compared with the 4AP/BIC value of WT (1-way ANOVA with Tukey's test). (*C*) EMSA revealed binding of CREB, MEF2, and SRF to the boxes *B*, *C*, and *D*. *Top*, the matched nucleotides are indicated by dots. The evolutionarily conserved nucleotides are highlighted in gray. The mutated nucleotides are shown with white letters. *Bottom*, representative results of EMSA. The brain nuclear extracts were added with probes of the boxes *B*, *C*, and *D*. Specific DNA-protein complexes (arrows) were observed, which disappeared by adding excessive amounts of unlabeled competitors (Comp), but not by mutated competitors (Mut Comp). Antibodies against CREB, MEF2, and SRF disrupted or supershifted the complexes, whereas a control antibody (anti-Myc) had no effects. (*D*) Chromatin immunoprecipitation (ChIP) assays revealed physical binding of CREB, MEF2, and SRF to SARE in the genome. Target genomic sequences were amplified with specific primer sets by qPCR. *Left*, the genomic region adjacent to the SARE sequence (within 200 bp) was detected in the immunoprecipitates obtained using an anti-CREB antibody, while a negative control sequence 10 kb downstream of SARE was not. The Somatostatin promoter was used as a positive control. *Middle*, detection of SARE in the immunoprecipitates obtained using an anti-MEF2 antibody. The Nur77 promoter was used as a positive control. *Right*, detection of SARE in the immunoprecipitates obtained using an anti-SRF antibody. The β-actin promoter was used as a positive control.

an RFP marker (TurboFP635) was driven under the control of a constitutive *pgk* promoter, while in the other, a d2EGFP reporter was expressed under the control of SARE-ArcMin. A control virus vector contained all these elements except for SARE (Fig. 5*A*).

BDNF is known to effectively induce endogenous Arc/Arg-3.1 expression in neurons. When SARE-ArcMin lentivirus-infected neurons were stimulated with BDNF, GFP signals became detectable in individual neurons (Fig. 5*B*). We further examined, by time-lapse live-cell fluorescence imaging, the activation time course of the genome-integrated SARE, upon high-frequency electrical

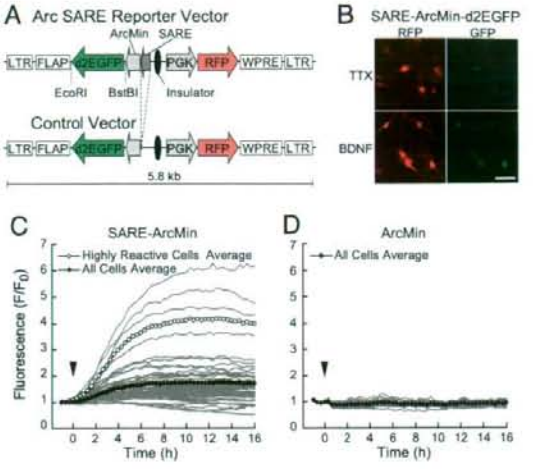

Fig. 5. Lentivirus-based genomic integration of the SARE reporter. (*A*) Design of lentiviral vectors. *Top*, the SARE reporter vector encodes an inducible reporter GFP (d2EGFP) under the control of SARE-ArcMin and a constitutively expressed infection marker RFP (TurboFP635) under the control of a *pgk* promoter. *Bottom*, a control vector lacking SARE. (*B*) Hippocampal neurons infected with the SARE reporter lentivirus were stimulated with BDNF for 6 h at 14 days postinfection. (Scale bar, 50 μm.) (*C*) GFP live-cell imaging of SARE-virus-infected neurons stimulated with high-frequency electrical pulses. Hippocampal neurons infected with the SARE reporter lentivirus were stimulated with field electrical pulses at time 0 h (triangle, 100 pulses at 100 Hz, 9 times), and GFP fluorescence was monitored. Gray lines, traces of individual neurons. Filled squares, the average trace of all neurons examined ($n = 59$). Open circles, the average trace of highly reactive neurons (top 10% of all neurons sorted by the F/F_0 value at the time of 8 h, $n = 6$). (*D*) No GFP fluorescence changes were observed in control-virus-infected neurons. Filled squares, the average trace of all neurons examined ($n = 18$).

stimulation (9 bursts of 100 Hz, 1 sec applied by field stimulation). In most of the SARE-ArcMin lentivirus-infected neurons, GFP fluorescence consistently increased immediately after the stimulation and started to saturate at ≈6–8 h (Fig. 5*C*), while the control virus-infected neurons showed virtually no GFP responses (Fig. 5*D*). Some of the neurons were particularly responsive (Fig. 5*C*), indicative of high copy number expression from multiple and/or transcriptionally favorable genomic loci. Alternatively, these neurons might have been favored because of their highly excitable properties within the neuronal network in culture as previously reported (10).

The above results suggested that the SARE-ArcMin lentivirus might provide a way to visualize specific sets of activated neurons in a given neural circuit in the brain. As a model, we designed an in vivo SARE-ArcMin reporter assay by directly injecting into mouse brains a d2EGFP reporter lentivirus. Consistent with prior reports (27), viral injection into the lateral ventricles of E15 mouse embryos reproducibly resulted in selective integration of infected neurons into layers 2/3 throughout the neocortex, as identified by RFP fluorescence and morphological criteria. No systematic differences were observed in the numbers of infected neurons between the 2 hemispheres. In our conditions, the infection rate was ranging 2–5% of the total cells in layers 2/3.

Cortical activity in the primary visual cortex (V1) was then stimulated by direct manipulation of the visual sensory inputs. Virus-infected mice (3–4 week-old) were sensory-deprived on 1 eye by suture, dark-reared for 1–3 days, and the intact open eye was exposed to light (Fig. 6*A*). Such sensory manipulation produced unilateral activation of the V1, as visualized by high immunoreactivities of endogenous Arc/Arg-3.1 at layers 2/3 and 4 in the